

State-of-the-Art Chamber Facility for Studying Atmospheric Aerosol Chemistry

DAVID R. COCKER III,[†]
RICHARD C. FLAGAN,[‡] AND
JOHN H. SEINFELD*[§]

Department of Environmental Engineering Science, Department of Chemical Engineering, and Department of Chemical Engineering and Division of Engineering and Applied Science, California Institute of Technology, Pasadena, California 91125

A state-of-the-art chamber facility is described for investigation of atmospheric aerosol chemistry. Dual 28 m³ FEP Teflon film chambers are used to simulate atmospheric conditions in which aerosol formation may occur. This facility provides the flexibility to investigate dark, single oxidant reactions as well as full photochemical simulations. This paper discusses the environmental control implemented as well as the gas-phase and aerosol-phase instrumentation used to monitor atmospheric aerosol formation and growth. Physical processes occurring in the chamber and procedures for estimating secondary organic aerosol formation during reaction are described. Aerosol formation and evolution protocols at varying relative humidity conditions are presented.

Introduction

Laboratory chambers are indispensable in the study of gas-phase atmospheric chemistry and atmospheric aerosol formation and growth. Because of the difficulty of isolating chemical and microphysical processes in the atmosphere from flow and mixing effects, chamber studies provide the means to develop mechanistic understanding of such processes. In this context, a laboratory chamber constitutes a well-mixed batch reactor in which the chemical processes of interest can be isolated directly.

From the point of view of atmospheric chemistry where chemistry is generally driven by sunlight, chambers can be divided into two categories: those driven by natural sunlight and those driven by artificial sunlight. The principal advantage of outdoor chambers is the availability of natural sunlight; disadvantages arise from varying light intensity resulting from atmospheric conditions and clouds as well as the general exposure to weather elements. Varying ambient conditions make replicate experiments difficult on a day-to-day basis and complicate temperature and relative humidity control. Indoor chambers afford precise control of temperature and humidity, but artificial lights may not simulate natural sunlight as closely as desired in portions of the solar spectrum, resulting in rates of certain photolysis reactions differing between the natural and artificial systems. Although not

identical to natural sunlight, artificial light allows for experiments to be repeated under identical photolytic conditions.

Although a reaction vessel with a volume of a few liters strictly qualifies as a "chamber", studies of atmospheric chemistry, especially involving aerosol formation, require systems of at least a few cubic meters in volume. Larger chambers reduce chamber surface area-to-volume ratios, thereby minimizing wall effects such as removal of gas-phase species and deposition of particles on the wall of the chamber.

Chamber studies of aerosol formation and growth combine the challenges of both gas-phase chemistry and aerosol dynamics. It is to this area that the present paper is directed. A principal goal of chamber-based atmospheric aerosol research is to understand the fundamental mechanisms by which gas-phase atmospheric chemistry leads to aerosol formation and growth. Measurements required in such experiments include gas-phase species concentrations and aerosol size distribution and composition. Measurements of aerosol microphysical properties, such as hygroscopic water uptake, are also useful.

We describe here a state-of-the-art indoor chamber facility for atmospheric aerosol research. Special emphasis has been placed on rapid, automated aerosol measurements. The system is particularly well suited for determination of the amount of secondary organic aerosol (SOA) formed from the oxidation of a single or group of parent hydrocarbons. Such experiments can be carried out in the absence or presence of a seed aerosol.

In this paper we describe the facility hardware and environmental controls. This is followed by a description of the gas-phase and aerosol-phase instrumentation. Details of aerosol formation and evolution experiments that probe the effects of relative humidity and the phase of the aerosol follow. Finally, a section is devoted to the aerosol dynamic processes occurring within the chamber.

Facility Overview

The indoor chamber facility comprises two 28 m³ Teflon chambers. The dimensions of each Teflon chamber are 2.5 × 3 × 3.7 m. The two chambers are suspended side-by-side in a 8.5 × 4.3 × 3.2 m room. Each chamber contains two Teflon ports, one port with a 0.3175 cm hole for gas chromatograph (GC) sampling and the other port with eight 0.9525 cm holes and one 2.54 cm hole that are used for sample injection and withdrawal. The chambers were manufactured by ATEC (Malibu, CA).

The chamber wall material is 2 mil (54 μm) FEP Teflon film, a transparent, nonreactive material. The wall material is flexible, enabling air extraction from the Teflon chamber without altering the pressure inside the reactor. The variation of light absorption by the Teflon material with wavelength, obtained at Caltech, is shown in Figure 1. A drawback of the use of Teflon film is static charge build-up on the FEP Teflon film surface that increases particle deposition to the walls.

Table 1 summarizes the instrumentation, while Figure 2 shows a block diagram of its configuration in the facility. Table 1 includes estimation of the accuracy or precision for each of the instruments. Each of the instruments will be discussed subsequently.

Three hundred 4-foot, 40 W Sylvania 350BL lights are used to illuminate the reaction chambers. The blacklight emission spectrum is displayed in Figure 3. To prevent heating at the surface of the Teflon film, the chamber is fixed at least 45 cm away from the chamber lights. To maximize the light intensity in the chamber, reflective Everbrite (Alcoa, PA) aluminum

* Corresponding author phone: (626)395-4635; fax: (626)796-2591; e-mail: seinfeld@caltech.edu.

[†] Department of Environmental Engineering Science.

[‡] Department of Chemical Engineering.

[§] Department of Chemical Engineering and Division of Engineering and Applied Science.

TABLE 1. Instrumentation Summary

instrument	measures	LDL/ range	accuracy	flow rate (LPM)	dedicated/ alternating
gas chromatograph flame ionization detector HP 5890 series II	reactive organic gas (ROG)	1 ppb ^a	2%	0.4	alternating
chemiluminescent NO _x analyzer Thermoenvironmental Instruments Model 42	NO, NO ₂	5 ppb	7%	0.7	alternating
ozone Dasibi Environmental hygrometer (capacitance probe) Vaisala HMP 233	ozone	1 ppb	4%	1.0	alternating
condensation particle counter TSI 3010 CPC	temperature	5–95%	0.50%	c	alternating
scanning electrical mobility spectrometer	relative humidity	–20 °C to 50 °C	0.1 °C		
tandem differential mobility analyzer	volume concentration	0.01 particles/cm ³	1% ^d	1.0	dedicated
portable spectroradiometer Licor – 1800	size distribution and number concentration	25–700 nm ^b	0.3% ^e	2.75	dedicated
gas chromatograph mass spectrometer HP GCD	hygroscopic growth factor	1.003	±0.003 ^e	2.75	alternating
	light spectrum	280–850 nm	0.1 nm	N/A	N/A
	ROG/gas-phase oxidation products	1 ppt ^a	5%	5.0	dedicated

^a Will be a function of hydrocarbon. ^b As currently configured. ^c In series with ozone and NO_x instruments. ^d 500–30 000 cm⁻³ as configured. ^e Measured precision.

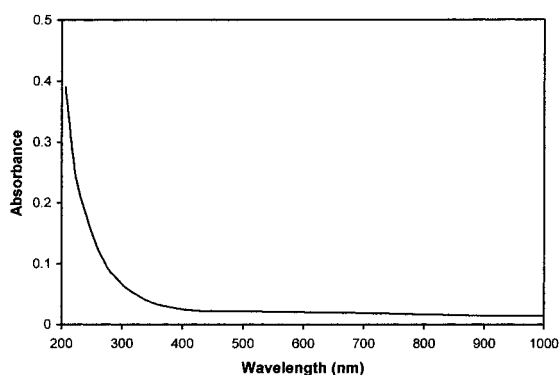


FIGURE 1. Absorption spectrum for 2 mil FEP Teflon film.

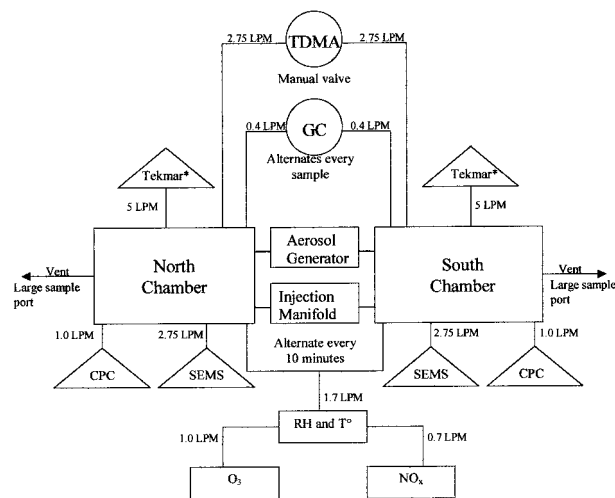


FIGURE 2. Block diagram of gas- and aerosol-phase instrumentation. *Tekmar refers to a Tenax-TA sampling tube which is later introduced to a GCD via a thermal desorption system.

sheeting (reflectance > 95%) covers all four walls, the ceiling, and the floor of the enclosure.

A Licor 1800 portable spectroradiometer is used to monitor the light spectrum emitted by the blacklights. The photolysis rate of NO₂ is estimated by steady-state actinometry, in which NO₂ is injected into a clean chamber and irradiated, and the resulting NO, NO₂, and ozone mixing ratios are measured. The photolysis rate constant, k_1 , is then estimated as $k_1 = k_3[O_3][NO]/[NO_2]$ where [O₃], [NO], and [NO₂] are concen-

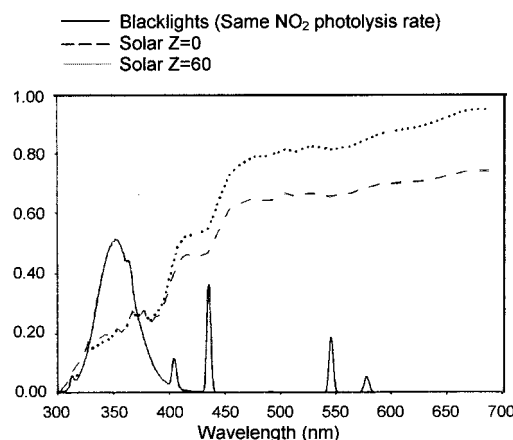


FIGURE 3. Light spectrum of Sylvania 350BL lights from Carter et al. (1). Solid line represents Sylvania 350BL; dashed line is solar light intensity at zenith angle = 0; dotted line is solar light intensity at zenith angle = 60. All three plots are normalized to have the same integrated NO₂ photolysis rate.

trations and k_3 (cm³/molecule/min) is the rate constant of NO and ozone reaction. The measured k_1 value (corrected for dark ozone plus NO reaction in the sampling lines) in the chamber at full light intensity is 1.5 min⁻¹, about three times that of natural sunlight at Pasadena, CA at a solar zenith angle of 0° on a clear day.

The artificial light produced by the blacklights is not representative of the entire ground-level solar light spectrum. A comparison of the relative light intensity of a typical fluorescent blacklight to ground-level solar radiation is given in Figure 3 (1). The ultraviolet irradiation produced by the blacklight lamps corresponds to the wavelengths for maximum NO₂ photolysis. However, the longer wavelengths that photolyze some organic compounds such as methyl glyoxal, in the range of 450–550 nm, are not emitted by the blacklight lamps. An extensive discussion of light sources and absorption cross sections for aldehydes and carbonyls is found in Carter et al. (1). Table 1 of Carter et. al (1) shows the relative rate of photolysis for several photolyzing species in the chamber when comparing blacklights to solar radiation. The blacklights used in the Caltech chamber are the same as those described in Carter et. al (1). It is important to note that the irradiation produced by blacklight lamps varies with manufacturer.

Compressed house air is forced through a series of packed bed scrubbers containing activated charcoal, silica gel, Purafil (Purafil Inc., GA), and molecular sieve, followed by a filter to produce dry, particle- and hydrocarbon-free air. This system supports flow rates in excess of 300 LPM producing particle-free air with NO_x, ozone, water vapor, and hydrocarbon levels below detection limits. A Millipore deionized water system produces 18.2 MΩ·cm (25 °C) water containing less than 0.02 EU/mL pyrogens, 2–5 ppb TOC, < 0.1 ppb silicates, < 0.1 ppb heavy metals, < 1 cfu/mL microorganisms, and 1 particle larger than 0.2 μm/mL for use as a solvent in aerosol seed generation and for chamber humidification.

A 52.8 kW heat exchanger controls the temperature of the insulated room housing the instrumentation and Teflon chambers. The temperature can be set from 18 °C to 50 °C with the chamber lights on and 15 °C to 50 °C with the chamber lights off. Temperature drift during an experiment rarely exceeds ± 0.5 °C with a transient in temperature of less than 1 °C for the time immediately following the blacklights being turned on. Heat generated by the blacklights is dispersed throughout the room using eight four-room (14.2 m³ min⁻¹) circulating fans. The instrumentation and sampling lines must be maintained at the chamber temperature to prevent perturbation of the sample during measurement so the instruments are located within the controlled temperature environment. The duration of the experiment ranges from 30 min to 24 h.

A 1500 W immersion heater submerged in > 18.2 MΩ·cm water in a 60 cm tall, 7.5 cm diameter glass cylinder fitted with a Teflon cap generates water vapor for chamber humidification. The steam passes through 2.5 cm diameter Teflon tubing into the chamber at a rate sufficient to achieve a relative humidity of 50% in approximately 40 min. A Vaisala (HMP233) capacitance meter measures relative humidity and temperature with stated temperature accuracy of ±0.1% and RH accuracy of ±0.5%. The water vapor addition does not introduce detectable particles or hydrocarbons into the chamber.

System Preparation

Thoroughly flushing the chamber with at least 10 chamber volumes of clean air over 24 h prior to the start of an experiment reduces ozone, NO_x, hydrocarbons, and particle concentrations below the detection limits of the instrumentation. Periodically the chamber walls are further cleaned by baking under blacklights at 50 °C while flushing with clean air.

Reactant Injection. Microliter syringes are used to measure and inject known volumes of liquid hydrocarbons (boiling point < 240 °C) into a 250 mL glass bulb. Gently heating the glass bulb with a heat gun vaporizes the hydrocarbon into an ultrapure air stream. The vapors pass through a FEP Teflon transfer line and a stainless steel port for injection into the chambers. Compounds with bp > 240 °C must be injected immediately adjacent to the injection port to minimize wall losses of the hydrocarbons before they reach the chamber.

Certified mixtures of gas-phase compounds in N₂ are introduced into the chamber using a mass-flow controller (Sierra Instruments Inc., CA) to maintain the flow-rate for a set period of time. The gas is then flushed into the chamber with ultrapure air through a FEP Teflon line and stainless steel port.

Seed Generation. Aerosol growth experiments frequently employ inorganic electrolyte seed aerosol. A stainless steel constant-rate atomizer (2) generates the seed aerosol from a 0.005 M solution of salt in ultrapure water. Dry (effloresced) aerosols are produced by passing the aerosol through a heated line and a Nafion diffusion dryer. Wet, deliquesced aerosols are injected by maintaining the RH of the injection line and

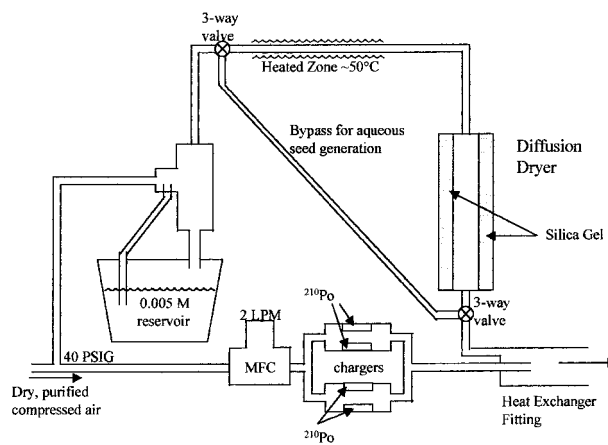


FIGURE 4. Seed particle generation system.

the chamber above the efflorescence RH of the salt. In each case, the seed aerosol is mixed, in a heat exchanger fitting, with air that has been passed through a ²¹⁰Po coated tube to eliminate the charge produced during atomization. The seed generation apparatus is shown in Figure 4.

Gas-Phase Instrumentation

A Hewlett-Packard 5890 series II Plus gas chromatograph (GC) equipped with a flame ionization detector (FID) monitors gas-phase hydrocarbon concentrations in the chamber. The GC employs a six-port gas injection valve for direct injection onto the GC column, DB-5 (J&W Scientific, CA) 60 m × 0.32 mm. A pump pulls the sample from the chamber through a 10 mL stainless steel sample loop at a rate of 0.4 LPM.

GC/FID measurements are taken every 11 min, alternating from one chamber to the other. The estimated uncertainty of the measurement is ±2%. A hexafluorobenzene (C₆F₆) tracer provides an internal standard for the GC measurements and serves as an indicator of air leaks in the chamber. This stable tracer does not react with hydroxyl radical, nitrate radical, or ozone at an appreciable rate. To calibrate the GC/FID for the parent hydrocarbon and C₆F₆, the parent hydrocarbons and C₆F₆ in a methylene chloride diluent are injected into a small Teflon chamber that is then filled with clean air at 5 LPM to a volume of 50 L. A minimum of three calibration measurements at each of four different concentrations is fit with a straight-line regression through zero.

A HP GCD (gas chromatograph with electron impact ionization, mass spectrometric detection) measures concentrations of vapor-phase hydrocarbons on samples collected downstream of a filter on Tenax TA adsorbent packed stainless steel tubes at a 5 LPM flow rate. A Tekmar-Dohrmann desorber instrument with cyrofocusing capabilities injects these samples into the GC column for gas-phase oxidation product identification and quantification of hydrocarbons that are difficult to introduce to the GC/FID through a conventional gas injection valve.

NO, NO₂, and NO_x mixing ratios are tracked using a Thermo Environmental Instruments Inc. (MA) Model 42 chemiluminescent NO–NO₂–NO_x analyzer. The analyzer continuously samples at a flow rate of 0.7 LPM, alternating between the chambers in ten-minute intervals. The instrument is calibrated weekly using a certified cylinder of NO. The accuracy of the measurement is ±7%.

A Dasibi Environmental (CA) nondispersive ultraviolet ozone analyzer monitors the chamber ozone concentration. The ozone analyzer samples at a rate of 1 LPM, pulling from alternating sides of the chamber in ten-minute intervals. The stated accuracy of the ozone instrument is ±4%.

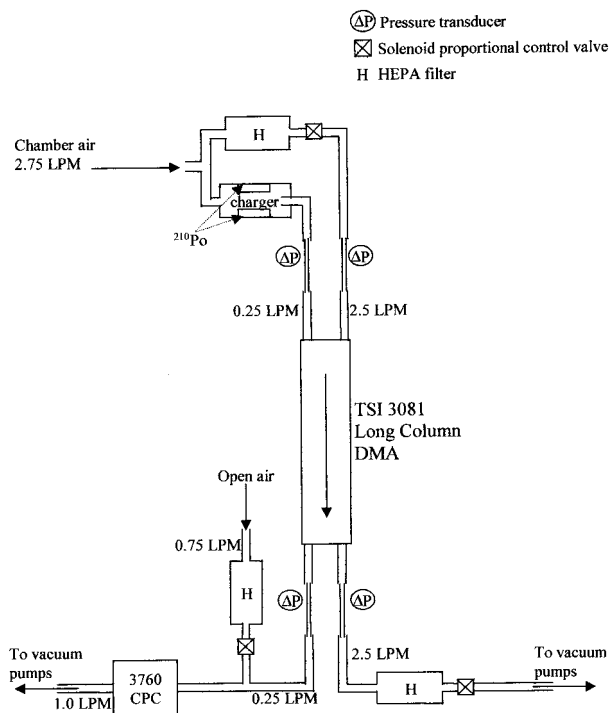


FIGURE 5. Automated scanning electrical mobility spectrometer. Pressure transducers monitored by computer; solenoid proportional control valves controlled by computer.

Aerosol Instrumentation

The aerosol instrumentation for the chamber includes a scanning electrical mobility spectrometer (SEMS), a tandem differential mobility analyzer (TDMA), and a condensation particle counter (CPC). Combined, these devices measure particle size distribution, aerosol number concentration, and the hygroscopic nature of the chamber aerosol. Duplicate aerosol-phase instruments continuously (except for the TDMA) sample from each side of the chamber at an average flow rate of 5.1 LPM.

Size Distribution Measurements. Particle size distributions and total number concentrations are obtained every 60 s using two scanning electrical mobility spectrometers (SEMS) (3), one for each side of the chamber (Figure 5). Each SEMS is equipped with a TSI model 3077 ⁸⁵Kr neutralizer, a TSI model 3081 long column cylindrical differential mobility analyzer (DMA), and a TSI model 3760 condensation particle counter (CPC). The DMAs operate with sheath and excess flows of 2.5 LPM and sample inlet and classified aerosol outlet flows of 0.25 LPM. Raising the DMA column voltage exponentially from -30 V to -7000 V enables measurement of the mobility spectrum of the aerosol over the mobility diameter range, 25–700 nm.

The volumetric flow rates and the potential applied to the inner rod of the DMA must be controlled precisely for accurate mobility measurements. A Bertan (NY) 602C that has been modified for linear output from -10 V to -10 000 V provides the rod potential. Laminar flow meters, consisting of a differential pressure transducer (Dwyer, IN, model 600-2) that measure the pressure drop across a laminar flow element, monitor the volumetric flow rates. Fifty milliliter jars filled with silica gel isolate the pressure transducers from potentially humid flows. The measured pressure drop is proportional to the volumetric flow rate. Solenoid proportional control valves (MKS model 248A) are used to adjust the flow rates on the particle-free flows, while the flow rates of all DMA flows are measured. This arrangement eliminates variable particle losses associated with aerosol passage through valves at different settings, while still ensuring precise flow settings.

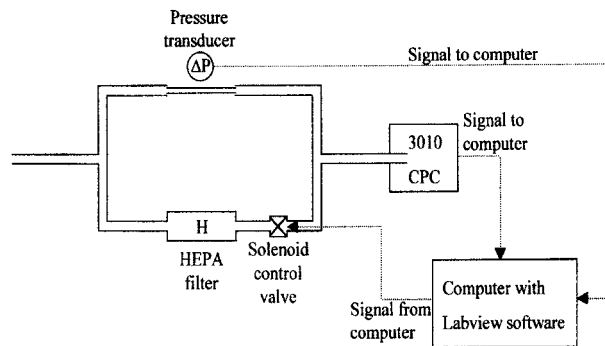


FIGURE 6. Condensation particle counter dilution system.

A personal computer (PC) using Labview software actively controls the volumetric flow rates and DMA voltage. An analog input board, a PC-LMP-16 PNP (National Instruments, Texas), monitors the flow rate, the column voltage (after a 2000:1 voltage divider), and the 3760 CPC counts. A digital/analog (D/A) output board, a PCI-6713 (National Instruments, TX), controls the solenoid valves and the high voltage supply. Software based proportional-integral-derivative (PID) control adjusts the three valves controlling the four DMA flows at a rate of 100 Hz, enabling flow rate control to $\pm 0.2\%$. A log-ratio amplifier (Burr-Brown model JP100) operated in anti-log configuration, exponentiates the linear, 12-bit precision analog voltage to drive the high voltage supply over the entire DMA range (10–10000 V) with a precision of $\pm 0.5\%$. The sampling line and SEMS system temperatures are maintained within 0.2 °C of the chamber temperature to prevent evaporation of or condensation on the aerosol during sampling. The sheath flow passes through a Teflon filter (CPPK Gelman) to minimize perturbations to the RH and gas-phase hydrocarbon species concentrations so that the aerosol passing through the DMA column will remain at equilibrium with the surrounding gas-phase.

A data inversion routine converts the count versus time data obtained from the SEMS by the PC to a size distribution and number concentration (4). The inversion routine accounts for the diffusional broadening of the DMA transfer functions, mixing-induced delays in counting particles by the CPC, the transmission efficiency of the aerosol stream through the sampling line and SEMS, and the charging efficiency of the neutralizer.

We have examined the reproducibility and stability of the SEMS measurement by continuously monitoring mobility classified (to eliminate solute particles) 198 nm polystyrene latex (PSL) spheres for 64 h. The diameter reported fluctuated by ± 0.5 nm over the entire duration of this test. Currently there is no calibration standard for volume concentration so only the precision for such measurement is added. After correcting for atomizer output drift using a parallel CPC to monitor the particle concentration variability in the aerosol volume concentration measurement was found to be less than 1%.

Number Concentration. Independent particle number concentrations are recorded using TSI model 3010 condensation particle counters to corroborate the DMA concentrations and to aid in estimating particle wall losses. Particle coincidence in the CPC was minimized by splitting the aerosol stream from the chamber, filtering 80% of the flow, and mixing the two streams so that only 1/5 of the aerosol stream reaches the CPC. This extends the measurement range of the CPC up to approximately 50 000 particles cm^{-3} . Figure 6 illustrates the CPC system.

Hygroscopicity Measurements. The tandem differential mobility analyzer (TDMA) provides a measure of the hygroscopic behavior of an aerosol. Figure 7 illustrates the experimental system based upon the original design of Rader

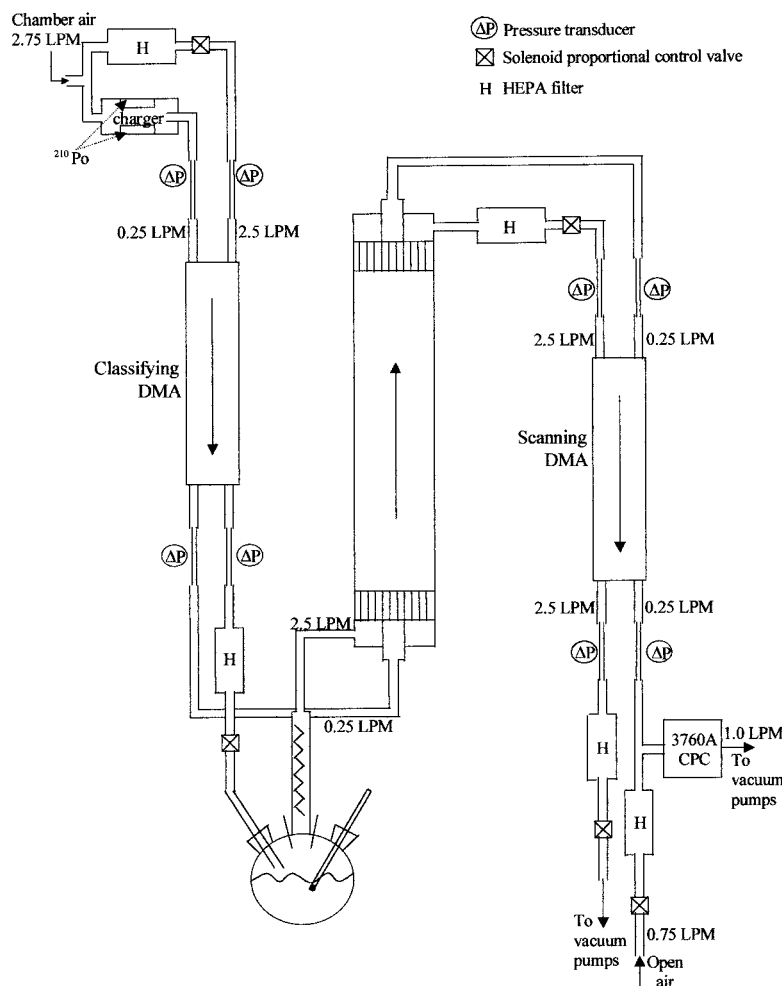


FIGURE 7. Tandem differential mobility analyzer system. Pressure transducers monitored by computer; solenoid proportional control valves controlled by computer.

and McMurry (5). It consists of two TSI 3081 long column cylindrical DMAs, a laminar flow environmental chamber, a ^{210}Po stainless steel neutralizer (Aerosol Dynamics, CA), and a TSI Model 3760A CPC. Flow rates of 2.5 LPM are used for both the sheath and excess flows and 0.25 LPM for both polydisperse and monodisperse flows. The ratio of the diameter of humidified aerosol to that of classified aerosol, $G_r = D_p(\text{humidified})/D_p(\text{dry})$, defines a measure of the water uptake of an aerosol known as the hygroscopic growth factor.

The first DMA in the TDMA system operates at constant voltage to extract particles in a narrow size range from a polydisperse aerosol sample. This classified aerosol then passes through a flow straightening tube before entering at the center of a humidification tube. Humid air enters coaxially to the sample. The 1003 mm length of the 47 mm diameter humidification tube is sufficient to ensure fully developed flow and a uniform distribution of water vapor across the tube. Centerline particle injection minimizes variations in the residence time, typically 10 s. An aerosol sample extracted from the centerline of the humidification tube then passes through a second DMA that is operated in scanning mode, i.e., as a SEMS, to measure the particle size distribution after humidification. Additional measurements made without humidification (bypassing the humidification tube) provide the data needed to calculate the growth factor. Both size distributions are fitted to log-normal distributions to facilitate calculation of G_r .

To minimize perturbations in the particle size during TDMA measurements, the temperature of the sampling lines and the entire TDMA instrument are maintained within ± 0.2

$^{\circ}\text{C}$ of the chamber temperature. The sheath flow for the first DMA is taken from the chamber and filtered with a Gelman CPPK filter to minimize RH fluctuations and maintain the chamber gas-phase organic composition in the system. Excess air from DMA1 is filtered and humidified by passing through a heated flask saturator containing ultrapure water and then through a condenser that controls the total gas-phase water concentration. Sheath air for the second DMA is filtered and taken from the laminar flow reactor to once again maintain RH and organic concentrations surrounding the particles. Flow and sizing calibrations account for the excess water-vapor volume added by humidification between the first and second DMA.

The system RH is controlled to within $\pm 0.5\%$ by a feedback loop between a digital hygrometer (Vaisala HMP233) and a refrigerated bath that controls the condenser temperature. A Labview-based PID controller maintains the flow within $\pm 0.5\%$. The larger uncertainty in flow rate results from simultaneous control of eight flows with five valves, compared to four flows with three valves in the SEMS. The data inversion process corrects for diffusional broadening in the transfer function, particle transmission efficiency, charging efficiency, and mixing effects in the CPC (4). A full scan takes 60 s. A typical size distribution is shown in Figure 8.

The TDMA was used to measure the hygroscopic G_r of the well-characterized salts, ammonium nitrate and ammonium bisulfate. Details of these measurements and their comparison to literature values and thermodynamic theory for these salts are reported in Cocker et. al (6).

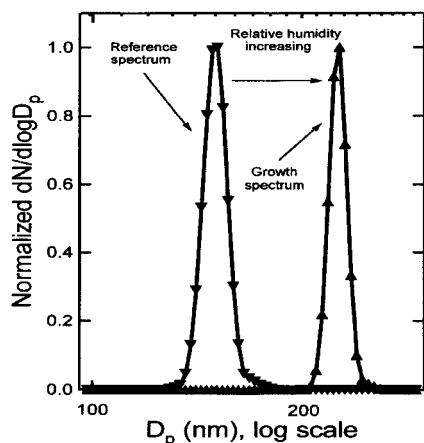


FIGURE 8. Sample TDMA size distribution spectrum. Left curve is output of second DMA for dry $(\text{NH}_4)_2\text{SO}_4$ seed particles classified to 136 nm by first DMA at RH = 0%. Right curve is output of second DMA for dry $(\text{NH}_4)_2\text{SO}_4$ seed particles classified to 136 nm by first DMA at RH = 85%.

Aerosol Formation and Evolution Experiments

In the absence of seed particles, aerosol may form by homogeneous nucleation. The number of particles that results depends strongly upon the operating conditions. Moreover, the concentration is uncertain since nucleation produces particles that are, at least initially, too small to detect. For quantitative measurements of aerosol yield, we therefore turn to seeded chamber studies. As described below, the aerosol yield varies depending on whether the seed particles are dry or not.

Dry Nucleation. In experiments performed without seed particles and at low relative humidity, aerosol forms when a gas-phase organic product accumulates to a sufficient supersaturation to induce homogeneous nucleation. Condensation and subsequent absorption of oxidation products leads to particles that are 100% organic in composition. The quantity of aerosol produced in this case, estimated from the final aerosol volume after accounting for wall losses, provides a measure of the SOA formation potential in a clean, dry environment. TDMA measurements of the chamber aerosol produced in the absence of seed particles reveals the hygroscopic nature of the pure organic oxidation products.

Humid Nucleation. In experiments performed at elevated RH, but without seed particles, aerosol also forms by nucleation, but subsequent particle growth involves partitioning of both water and organic products into the aerosol. Used in conjunction with a dry nucleation experiment, the humid nucleation experiment allows one to explore the effects of the presence of water on gas-particle conversion. The SOA yield of the wet nucleation experiments can be corrected for water uptake by estimating the water fraction as that obtained from TDMA analysis of dry nucleation particles. The SOA yield in the humid system can be calculated and compared to the dry nucleation experiments after accounting for wall losses.

Dry Seed, Dry Conditions. In experiments performed with sufficiently high concentrations of water-free inorganic seed particles in a dry chamber, the seed particles suppress nucleation and ensure that the chamber aerosol lies within the size range of the instrumentation throughout the experiment. SOA production commences when a sufficient supersaturation of oxidation products accumulates to induce the condensation onto the dry seed surface producing an initial organic layer. Further aerosol growth occurs by absorption of reaction products into the organic layer. The resulting aerosol contains both inorganic and organic species. With a nonvolatile seed aerosol, the total suspended inorganic

aerosol volume changes only by particle depositions onto the chamber walls. Therefore, the organic aerosol yield can be computed from the total aerosol produced less the initial amount of inorganic material present after correction for wall losses. Comparison of the results of these experiments to those of dry nucleation experiments allows one to estimate the influence of a dry, inert nonreactive surface on gas-particle partitioning.

Dry Seed, Elevated Relative Humidity. These experiments add the influence of water vapor to the previous experiments. To keep the seed particles dry, the RH in these experiments cannot exceed the deliquescence RH of the inorganic salt comprising the seed particles. Aerosol growth takes place when a sufficient supersaturation of oxidation products leads to the production of an initial organic layer. Further aerosol growth occurs as water and organic material partition into the organic or organic-water phase. The resulting aerosol contains inorganic material, organic material, and, possibly, water. Several investigations have noted that the deliquescence RH of the inorganic salt is unperturbed by organic coatings (7). If, therefore, the inorganic core of the aerosol remains dry, SOA yield can be measured as the final aerosol volume less the initial seed volume and water content (all corrected for wall losses). Water content is again measured independently by TDMA analysis either using dry aerosol from dry nucleation or from dry seed, low RH experiments.

Care must be taken to ensure that the aerosol is dry when injected and is never exposed to RH higher than the particle deliquescence RH. The state of the seed aerosol is verified prior to the start of an experiment through TDMA analysis at an RH above the seed deliquescence RH. A G_f value lower than that for a dry seed aerosol indicates that the seed is not dry.

Aqueous Seed, Elevated Relative Humidity. In this case, experiments are performed at elevated RH with deliquesced (wet) seed aerosol. Generation of such aerosol requires that at no point does the RH surrounding the aerosol drop below its efflorescence RH. The state of the aerosol can be verified by TDMA measurements of the hygroscopic growth factor of the particles. The water content of the inorganic seed can be estimated based on thermodynamic theory (8). Oxidation products may partition into the aqueous phase or into a separate organic phase. The amount of water in the aerosol may either increase or decrease during growth. Because the final aerosol water content cannot be independently determined, the total aerosol yield, including water and organic material, is reported.

Aerosol Dynamics

A major goal of the aerosol chamber experiments we have described is to determine the aerosol formation potential of either a single compound or a mixture. To do this, one must estimate the mass of aerosol produced over the course of an experiment. Figure 9 shows a typical set of data, including the hydrocarbon disappearance, the amount of suspended aerosol volume, and the number distribution of particles. The reaction is considered finished when the aerosol volume (corrected for wall processes) is no longer changing. Several microphysical processes occurring in the chamber must be considered in order to estimate the amount of organic aerosol produced (9).

The principal process that complicates the interpretation of measured aerosol data is loss of particles to the wall of the chamber. To determine the total amount of aerosol mass generated, one must estimate the quantity of the aerosol lost to the chamber walls over the course of the experiment and add that to that measured of the end of the run. Particles deposit on the wall at a rate that is proportional to the particle concentrations and depends on particle size, leading to first-

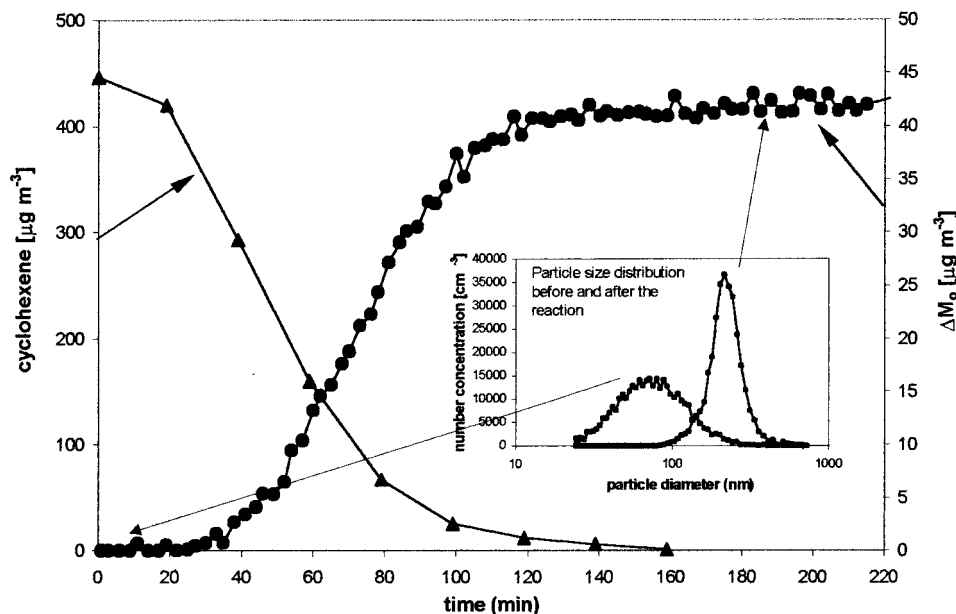


FIGURE 9. Cyclohexene and organic aerosol mass as a function of time. Chamber initially seeded with ammonium sulfate. As the cyclohexene concentration decreases with time, the organic aerosol mass increases correspondingly. The organic aerosol mass, ΔM_o , is calculated from the change in aerosol size distribution (shown in insert) and accounts for wall deposition. ΔM_o is the total aerosol mass produced during the experiment.

TABLE 2. Characteristic Time Scales for Processes Occurring in the Chamber^a

process	time constant	typical chamber values
formation of condensable gas	$\tau_F = \frac{1}{k_{OH}[OH]}$	2 h
gas-particle transport (condensation)	$\tau_{GP} = \frac{1 + 8\lambda/\alpha D_p}{2\pi N D_p \lambda c}$	2 min
particle-wall transport (wall deposition)	$\tau_{PW} = \frac{1}{(A_c/V_c)k_{MP}}$	5 h
gas-deposited particle transport (absorption to deposited aerosol)	$\tau_{GD} = \frac{1}{\alpha(A_p/V_c)k_{MG}}$	3.5 d
coagulation (no nucleation)	$\tau_{COAG} = \frac{2}{K_{ij}N}$	3.1 d
coagulation (nucleation)	$\tau_{COAG} = \frac{2}{K_{ij}N}$	200 s at 10^7 particle cm^{-3} to 56 h at 10^4 particle cm^{-3}

^a If transport to particle \gg formation of condensable gases; $k_{OH} = 2 \times 10^{-11}$ $\text{cm}^3/\text{molecule}\cdot\text{s}$, a typical first-order hydroxyl reaction rate constant; $[OH] = 7 \times 10^6$ $\text{molecule}/\text{cm}^3$, concentration of hydroxyl radical; $N = 1 \times 10^4$ cm^{-3} , particle number concentration; $D_p = 100$ nm, particle diameter $\alpha = 1.0$, sticking probability; $\lambda = 65.1$ nm, mean free path; $c = 600$ m/s, velocity of semivolatile gas molecule; $(A_c/V_c) = 1.0$ m^{-1} , chamber surface area-to-volume ratio; $k_{MG} = 1.0$ m/min, mass transfer coefficient for condensing species to particles adsorbed to chamber surface; $k_{MP} = 1.5 \times 10^{-3}$ m/min, mass transfer coefficient for particles to chamber surface; $A_p/V_c = 2 \times 10^{-4}$, ratio of surface area of particles deposited on chamber wall to chamber volume; K_{ij} for $N = 1 \times 10^4$ cm^{-3} , $D_p = 100$ nm (K_{ij} is particle-particle collision frequency).

order kinetics, i.e.

$$\frac{dN(D_p, t)}{dt} = -\beta(D_p)N(D_p, t) \quad (1)$$

where $\beta(D_p)$ is the wall loss coefficient, $N(D_p, t)$ is the particle number concentration, and D_p is the particle diameter (9). β values are estimated from particle number concentration versus time data for each experiment using the above equation. Values of β for typical particle sizes in our chamber range from 0.0015 to 0.003 min^{-1} . The observed decay in total number concentration provides an estimate of the amount of aerosol lost to the wall over the course of an experiment. The only competing process that can confound

this interpretation is particle-particle coagulation that also reduces the particle number concentration. In seeded experiments, at typical seed aerosol size (about 100 nm in diameter) and number concentrations (about 10^4 cm^{-3}), the time scale for coagulation is about 74 h; consequently, coagulation can be neglected as a cause of the decrease in the aerosol number concentration when seed aerosol is used.

In the absence of seed aerosol, initial particle formation occurs by nucleation. Typically, nucleation occurs in a brief burst that produces 10^4 – 10^7 particles cm^{-3} . At number concentrations of 10^7 , 10^6 , 10^5 , and 10^4 particles cm^{-3} , the time scale for coagulation is on the order of 200 s, 33 min, 5.6 h, and 56 h, respectively. Therefore, for large nucleation bursts, coagulation becomes a significant process to reduce

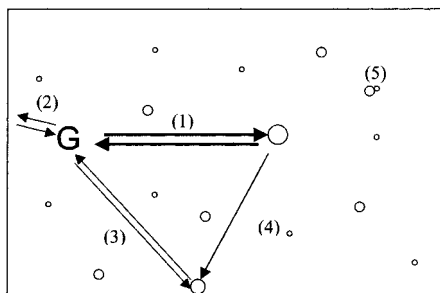


FIGURE 10. Illustration of different processes occurring within the chamber. Pathways include the following: (1) condensation, (2) gas-phase wall adsorption, (3) gas-deposited particle transport, (4) particle-wall transport, and (5) coagulation.

the number concentration. Because coagulation is a second-order process, the rate of reduction in the number concentration by coagulation decreases much more rapidly than does particle loss to the walls.

Table 2 gives characteristic times for chamber processes important in gas-to-particle conversion. Note that the only significant change in particle number concentration occurs through wall deposition processes (except when nucleation occurs). Therefore, the number of particles in the chamber can be described by the first-order wall loss rate as $N = N_0 e^{-\beta t}$. As the mass transfer rate to suspended particles greatly exceeds that of those deposited on the wall, the amount of organic material associated with each particle at the time of deposition is assumed to be constant. Thus, the total organic material produced is estimated to be the sum of that still suspended in the aerosol phase plus that deposited to the wall. The particle size increases due to condensation of organic vapors (and any nucleation products). The final size of the particles less the initial size of the seed particles provides an estimate of the volume of organic material suspended in the chamber. Figure 10 illustrates the competing processes. Adsorption of gas-phase compounds on the wall might possibly decrease their concentrations since the characteristic

time for diffusion to the wall of the present chamber is 1 min. However, FEP Teflon film is nonabsorptive to most hydrocarbons; measured losses of C_6F_6 and *m*-xylene are 0.001 h^{-1} (loss rate includes potential leaks).

Acknowledgments

This work was supported by the U.S. Environmental Protection Agency Center on Airborne Organics and U.S. Environmental Protection Agency Agreement CR827331-01-0.

Literature Cited

- (1) Carter, W. P. L.; Luo, D.; Malkina, I. L.; Pierce, J. A. *Environmental chamber studies of atmospheric reactivities of volatile organic compounds. Effects of varying chamber and light source*; Final report to National Renewable Energy Laboratory; 1995 (<http://cert.ucr.edu/~carter/absts.htm#explrept>).
- (2) Liu, B. Y. H.; Lee, K. W. An aerosol generator of high stability. *Am. Ind. Hyg. J.* **1975**, *861*–865.
- (3) Wang, S. C.; Flagan, R. C. Scanning electrical mobility analyzer. *J. Aerosol Sci.* **1989**, *8*, 1485–1488.
- (4) Collins, D. R.; Flagan, R. C.; Seinfeld, J. H. Improved inversion of scanning DMA data. *Aerosol Sci. Technol.* **2001**, In press.
- (5) Rader, D. J.; McMurry, P. H. Application of the tandem differential mobility analyzer to studies of droplet growth or evaporation. *J. Aerosol Sci.* **1986**, *17*, 771–787.
- (6) Cocker, D. R.; Clegg, S. L.; Flagan, R. C.; Seinfeld, J. H. The effect of water on gas-particle partitioning of secondary organic aerosol: I. α -pinene ozone system. *Atmos. Environ.* **2001**, In press.
- (7) Cruz, C. N.; Pandis, S. N. Deliquescence and hygroscopic growth of mixed inorganic-organic atmospheric aerosol. *Environ. Sci. Technol.* **2000**, *34*, 4313–4319.
- (8) Nenes, A.; Pandis, S. N.; Pilinis, C. ISORROPIA: A new thermodynamic equilibrium model for multiphase multicomponent inorganic aerosols. *Aquat. Geochem.* **1998**, *4*, 123–152.
- (9) Bowman, F. M.; Odum, J. R.; Seinfeld, J. H.; Pandis, S. N. Mathematical model for gas-particle partitioning of secondary organic aerosols. *Atmos. Environ.* **1997**, *31*, 3921–3931.

Received for review November 29, 2000. Revised manuscript received April 3, 2001. Accepted April 5, 2001.

ES0019169